Comparison of theory and experiment for elastic-plastic plane-strain crack growth

L. Hermann and J. R. Rice

Recent theoretical results on elastic–plastic plane-strain crack growth are reviewed and experimental results for crack growth in a 4140 steel are discussed in terms of the theoretical concepts. The theory is based on a recent asymptotic analysis of crack surface opening and strain distributions at a quasistatically advancing crack tip in an ideally plastic solid. The analysis is incomplete in that some of the parameters which appear in it are known only approximately, especially at large-scale yielding. Nevertheless, it is sufficient for the derivation of a relation between the imposed loading and amount of crack growth prior to general yielding, based on the assumption that a geometrically similar near-tip crack profile is maintained during growth. The resulting predictions for the variation of J with crack growth are found to fit well to the experimental results obtained on deeply cracked compact specimens.

L. Hermann, Ing, MS, and J. R. Rice, BS, MS, PhD, are with the Division of Engineering, Brown University, Providence, USA.

A recent theoretical analysis by Rice *et al.*[1] described the plane-strain elastic–plastic deformation and stress field very near the tip of a continuously growing crack in a non-hardening solid, obeying the Huber–von Mises yield condition and associated flow rule (i.e. the 'Prandtl–Reuss' equations). By requiring, as a possible criterion for quasistatic crack growth, that a geometrically similar profile of crack surface opening be maintained very near the tip, the analysis led to predictions of the manner in which crack length should vary with applied load during growth. The work described is an extension of earlier work by Rice and Sorensen,[2] and includes a correction to the form of the near-tip deformation and stress field presented in the latter. In both studies[1,2] the theoretical analysis is incomplete in that certain parameters or functions which appear in asymptotic expressions for the near-tip deformation field must be determined from full numerical elastic–plastic solutions for growing cracks. This has been done approximately by comparison with finite element solutions for the case of crack growth under well contained plastic yielding. Results for large-scale and general yielding are not yet available, although some discussion of the fully yielded case has been possible[1] by use of dimensional considerations and comparison with rigid–plastic slip-line solutions.

Our purpose here is to present experimental results on crack growth in a high-strength steel and to use these as a basis for comparison with the theoretical predictions mentioned above.

THEORETICAL ANALYSIS OF GROWING CRACKS

Figure 1*a* Shows the Prandtl slip-line field which describes the plane-strain near-tip stress state (at least when large changes in crack-tip geometry are neglected; *see* Rice and Johnson[3] and McMeeking[4]) for a non-growing crack subjected to monotonically increasing load under conditions of well contained yielding. This field may also apply at large-scale and general yielding in certain highly constrained configurations. During processes of stable crack growth, for which the applied load varies continuously with crack length a, a slightly different stress field results very near the tip. This was described by Rice *et al.*[1] and its slip-line interpretation is shown in Fig. 1*b*. In this case an elastic unloading sector develops between the centred fan region C and the back constant stress yield region B. The angles θ_1 and θ_2 depend somewhat on the Poisson ratio but are $\theta_1 = 115°$ and $\theta_2 = 163°$ for $\nu = 0{\cdot}3$. Remarkably, the stresses ahead of the crack differ only by about 1% from those for the Prandtl field of Fig. 1*a*.

Letting δ be the opening displacement between the upper and lower crack surfaces, the analysis shows that

$$\dot{\delta} = \alpha\dot{J}/\sigma_0 + (\beta\dot{a}\sigma_0/E)\ln[R/(a-x)] \quad (1)$$

very near the tip of a continuously growing crack (i.e. as $x \to a$, where x is the position along the crack). In this expression the superimposed dots denote time rates, σ_0 is the ideally plastic tensile strength, E the elastic tensile modulus, and β is dependent on Poisson's ratio, having the value[1] $\beta = 5{\cdot}08$ for $\nu = 0{\cdot}3$. Also, the intensity of the applied loading is, without loss of generality, phrased in terms of J (associated with the J-integral although as will be discussed, equation (1) remains valid for different ways of defining $\dot{J}$; the different choices imply different values for the parameter R).

In fact, α and R in equation (1) are not determined by the asymptotic analysis leading, for example, to the stress field of Fig. 1*b*. These parameters must be determined by comparison of equation (1) with complete elastic–plastic solutions for growing cracks, which are necessarily numerical and subject to uncertainties as to accuracy and interpretation very near the tip. We discuss each parameter in turn. First, α is dimensionless and might be expected to be rather close in value to the parameter α^* as defined by

$$\mathrm{d}\delta_{\mathrm{tip}} = \alpha^* \,\mathrm{d}J/\sigma_0 \quad (\dot{a} = 0) \quad (2)$$

for the crack tip opening displacement of a non-growing crack subject to monotonic load increase. This expectation seems to be confirmed by results of numerical solutions for crack growth under well contained plastic yielding. Letting 'ssy' denote small-scale yielding, it was found[1,2] that to within 5 to 10% accuracy $\alpha_{\mathrm{ssy}} \approx \alpha^*_{\mathrm{ssy}}$ where $\alpha^*_{\mathrm{ssy}} = 0{\cdot}65$. The parameter α may vary from α_{ssy} as large-scale and general yielding conditions are approached. For example, the

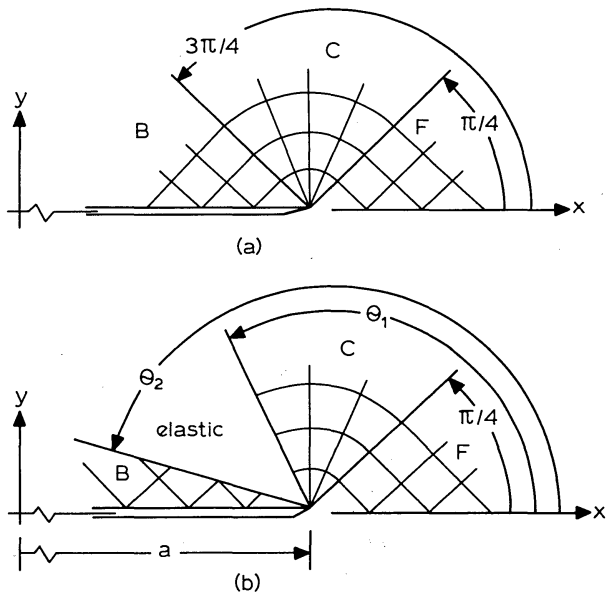

1 Slip-line representation of crack tip stress state: *a* for non-growing crack; *b* for growing crack

deeply cracked plane-strain bending configuration (Fig. 2) leads at fully plastic (fp) conditions to[1,5,6] $\alpha^*_{fp} = 0{\cdot}51$. Furthermore, $\alpha_{fp} = \alpha^*_{fp}$ *exactly* for the *rigid*–ideally plastic material model, so that it may be presumed that $\alpha_{fp} \approx \alpha^*_{fp} = 0{\cdot}51$ for elastic–plastic deeply cracked bend specimens which are loaded well into the plastic range. In fact, estimates of α^* from elastic–plastic solutions for non-growing cracks[5,7,8] suggest that α^* remains very close to $\alpha^*_{ssy}(= 0{\cdot}65)$ until the applied moment M per unit thickness approaches closely to the fully plastic limit moment,[1,6] $M_0 = 0{\cdot}364\sigma_0 b^2$, and then α^* decreases rapidly towards $\alpha^*_{fp}(= 0{\cdot}51)$ as deformation continues.

The parameter R in equation (1) evidently has dimensions of length, and it is reasonable to expect that R should have a value in approximate proportion to the size of the plastic region, or at least to the size over which stress distributions similar to those of Fig. 1 prevail. This notion has limited confirmation from comparisons of equation (1) with numerical simulations of crack growth under small-scale yielding. Such studies suggest that[1]

$$R \approx 0{\cdot}23EJ/\sigma_0^2 \quad . \quad . \quad . \quad . \quad . \quad . \quad . \quad . \quad . \quad . \quad . \quad . \quad . \quad (3)$$

for small-scale yielding where J has been identified as the far-field value of the contour integral taken in elastic material and hence equal to $G \equiv (1-\nu^2)K^2/E$ in the small-scale yielding limit. The value of R given by equation (3) is proportional to, but approximately 15 to 30% larger than, the maximum radius of the plastic zone under small-scale yielding conditions. The accuracy of equation (3) remains an open question; there may be some small dependence of R on the ratio of the length of crack growth to the size of the yield zone, but numerical solutions have not as yet been sufficient to resolve this.

Certainly, R must be expected to deviate from equation (3) as large-scale and fully plastic yielding conditions are reached. As discussed by Rice *et al.*[1] the behaviour of R at large-scale yielding cannot be decoupled from the definition of J; if J is defined so that in the limit of rigid–plastic response $(E/\sigma_0 \to \infty)$ $\dot{J}$ does not depend on $\dot{a}$ (but only on a and on the rate of imposed boundary displacement), then R might still be expected to have values in proportion with the size of the fan-like stress region. Hence, with an appropriate definition of $\dot{J}$, it was suggested[1] that for a configuration similar to that in Fig. 2 R might ultimately reach a limiting value of some definite fraction of the uncracked ligament dimension b. Suitable theoretical confirmation of this expectation (perhaps from numerical solutions) is lacking at present, and our experiments suggest that the large-scale yielding behaviour of R may be somewhat more complicated.

A possible criterion for stable crack growth has been developed from equation (1) in the following way. By integration, the form of the crack profile very near the tip can be written as

$$\delta = (\alpha r/\sigma_0)\,\mathrm{d}J/\mathrm{d}a + (\beta r\sigma_0/E)\ln(eR/r) \quad . \quad . \quad . \quad . \quad . \quad (4)$$

where $e = 2{\cdot}718$ is the natural logarithm base and $r = a - x$. The equation is asymptotically valid as $r \to 0$ for a continuously growing crack (i.e. when $\mathrm{d}J/\mathrm{d}a$ is finite). The expression can be rewritten as

$$\delta = (\beta r\sigma_0/E)\ln(\rho/r) \quad . \quad . \quad . \quad . \quad . \quad . \quad . \quad . \quad . \quad . \quad . \quad . \quad (5)$$

where

$$\rho = eR\exp[(\alpha/\beta)(E/\sigma_0^2)\,\mathrm{d}J/\mathrm{d}a] \quad . \quad . \quad . \quad . \quad . \quad . \quad . \quad . \quad (6)$$

It is clear from equation (5) that the form of the crack profile very near the tip is dependent only on the single parameter ρ. Hence, if one adopts as a possible fracture criterion the premise that the crack maintains a steady near-tip geometrical profile during growth, this is seen from equation (5) to be tantamount to assuming a crack growth criterion in the form

$$\rho = \text{constant} \quad . \quad . \quad . \quad . \quad . \quad . \quad . \quad . \quad . \quad . \quad . \quad . \quad . \quad (7)$$

Thus, with ρ understood to be constant, equation (6) is equivalent to the differential equation

$$\mathrm{d}J/\mathrm{d}a = (\beta/\alpha)(\sigma_0^2/E)\ln(\rho/eR) \quad . \quad . \quad . \quad . \quad . \quad . \quad . \quad . \quad (8)$$

which governs the variation of J with a during quasistatic crack growth. This is a 'differential equation' in the sense that R is dependent (in a way yet to be fully documented, at least beyond the small-scale yielding result of equation (3)) on J and probably on the previous crack growth.

Integrals of equation (8) have been presented in previous work[1] for crack growth under small-scale yielding, using equation (3) for R. In this case the J versus a relationship is determined fully by the initial value of J (i.e. J_{1C}) at the onset of growth and by the parameter ρ; J increases from J_{1C} with ongoing crack growth but ultimately approaches a limiting value (which makes $R = \rho/e$, so that $\mathrm{d}J/\mathrm{d}a = 0$) at

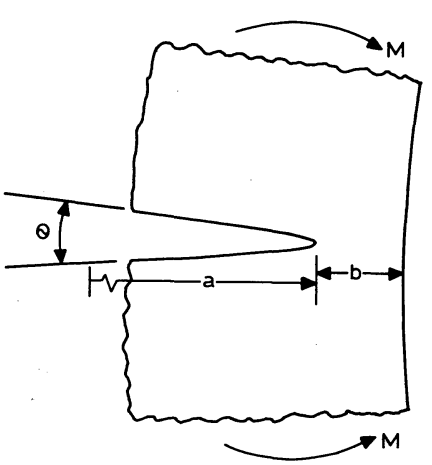

2 Deeply cracked plane-strain bending specimen

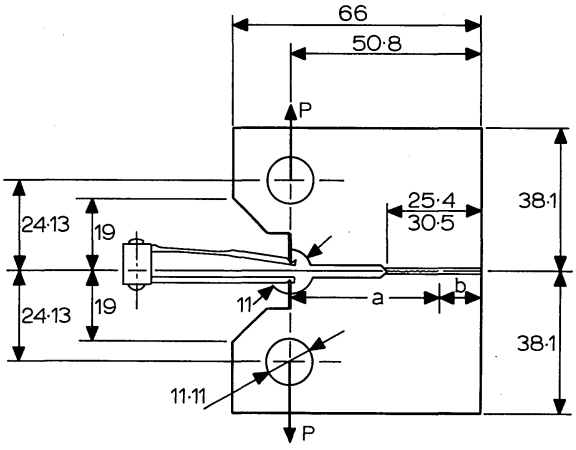

3 Specimen, with dimensions shown in mm, and clip gauge

which continuing crack growth can occur without further increase of J. This limiting value in the steady state has been denoted $(J)_{ss}$ in the previous work[1,2] and $(J)_{ss} = 1{\cdot}60\sigma_0^2\rho/E$.

A number of comments are pertinent. First, it is of interest to note that in order to maintain a steady geometrical profile near the crack tip, J must in general *vary* during crack growth (unless the size parameter R has reached the value ρ/e). This is a plasticity effect, traceable to the strain-path-dependent nature of elastic–plastic stress/strain relationships, in particular to the difference in response stiffness for plastic loading versus elastic unloading. It would not result in a non-linear elastic material even if that material had the same stress/strain relation for monotonic loading as does the elastic–plastic material. Instead, in such a non-linear elastic material the requirement of a constant near-tip crack profile during growth would be essentially equivalent to the requirement of a constant value of J during growth.

Second, the crack growth criterion of equations (7) and (8) is based on maintaining, in a sense, a fixed deformation state very near the crack tip during growth. This may be expected to provide a suitable model for ductile crack growth at least in circumstances for which significant void nucleation occurs only very near the tip, within the region of the fixed deformation state. It cannot be expected to apply with much precision in cases for which microcrack or cavity nucleation is influenced by the size scale in the material over which high stresses act. Obviously, the growth criterion also does not incorporate the physics of transition of a stable ductile tearing mode fracture to a cleavage mode fracture, which is presumably due to strain-rate elevations of local stress levels during quasistable growth processes with consequent change of microscopic fracture mode.

Third, it is of interest to note that the general form of the growth criterion seems to be independent of the manner in which the notion of a fixed near-tip deformation state is characterized. For example, Rice *et al.*[1] show that the equivalent plastic shear strain at points within the fan of Fig. 1*b* at small distances r directly above or below the crack tip is

$$\gamma^p = (m/\sigma_0)\,\mathrm{d}J/\mathrm{d}a + 1{\cdot}88(2-\nu)(\sigma_0/E)\ln(L/r) \quad . \quad . \quad . \quad (9)$$

for a continuously growing crack, where the parameters m (analogous to α of equation (4)) and L (analogous to eR) are also undetermined by the asymptotic analyses. The determination of these parameters from numerical solutions requires that local strains be known accurately; no results with the requisite accuracy are available at present. Nevertheless, it is clear that equation (9) can be rephrased in the form

$$\gamma^p = 1{\cdot}88(2-\nu)(\sigma_0/E)\ln(\zeta/r) \quad . \quad . \quad . \quad . \quad . \quad . \quad . \quad . \quad (10)$$

where

$$\zeta = L\exp\{[m/1{\cdot}88(2-\nu)](E/\sigma_0^2)\,\mathrm{d}J/\mathrm{d}a\} \quad . \quad . \quad . \quad . \quad (11)$$

and ζ measures the strength of the near-tip strain field. Hence, the criterion for crack growth with a fixed strain state prevailing very near the tip can be phrased as the requirement that $\zeta =$ constant, and this leads to a differential equation governing crack growth which is similar in form to that of equation (8).

Fourth, it is emphasized that the theoretical analysis leading, e.g. to equations (1, 4, 9) is based on an ideally plastic material. We can account for actual strain hardening in a very approximate manner by identifying σ_0 in equations (1, 2, 4–6, 8) as the ultimate (nominal) tensile strength σ_u. This is done in analysing the experiments (although in equation (3) for R we shall interpret σ_0 as the actual yield stress σ_y, which is reasonable if R is to be associated with the size of the plastic region). Nevertheless, more subtle strain-hardening effects than are revealed in the uniaxial tensile test can occur and may be relevant to the analysis of crack growth. These are related to the development of severe shape changes of the plastic yield surface (in stress–space). A special case is the development of a pointed vertex structure on the yield surface at the current stress state. This greatly reduced the stiffness of elastic–plastic response along non-proportional stressing paths, compared to predictions based on yield surfaces which do not change in shape and hence might be expected to be critical to the analysis of deformation fields near growing cracks. Remarkably, however, a recent analysis of steady-state Mode III crack growth by Dean and Hutchinson[9] shows very little difference between the crack surface displacements predicted according to a vertex yield model and to a model which retains the Huber–von Mises shape of the yield locus (i.e. 'isotropic' hardening). Whether effects of changes of yield surface shape are similarly without major effects for growing tensile cracks remains to be seen.

EXPERIMENTS

The material used in the experiments was an Al–Si killed AISI 4140 supplied as 19 mm thick plate by Bethlehem Steel Corporation. Compositional weight percentages are: 0·42C, 0·004P, 0·014S, 0·22Mo, 0·001As, 0·01Sb, 0·002Sn. The material was austenitized in argon for 1 h at 1140 K, oil quenched, and tempered for 1 h at 770 K, resulting in nominal tensile yield and ultimate strengths of $\sigma_y = 1173$ MN m^{-2} and $\sigma_u = 1327$ MN m^{-2}, respectively.

Four specimens were prepared, each with in-plane dimensions as shown in Fig. 3 (the larger dimension, 30·5 mm, for the distance from the notch tip to specimen back surface applies for specimen 4 only). The specimens were side-grooved in a shallow 90° V-notch shape to suppress shear lips, and were pre-fatigue cracked so that the remaining uncracked ligament b had values at the start of the ductile crack growth tests as shown in Table 1. This table also shows the thicknesses and side groove depths; thicknesses listed are the average of those before and after side-grooving, and are used to reduce measured loads to loads per unit thickness for use in theoretical formulae. The uncracked ligaments b are small compared to overall specimen dimensions and hence for analytical purposes the specimens are modelled as deeply cracked bend specimens

Table 1 Specimen ligament sizes, thicknesses, and side-groove depths (for other dimensions see Fig. 3)

Specimen number	Initial ligament size b_0, mm	Thickness (average), mm	Side-groove depth, mm
1	10·75	12·19	0·51
2	10·42	15·37	0·51
3	10·62	18·54	0·76
4	15·86	18·54	0·76

(Fig. 2) with M computed about the mid-point of the uncracked ligament. Thus, $M = P(a+b/2)$ and increments $d\theta$ of the rotation measure in Fig. 2 are identified as $d\theta = d\Delta/(a+b/2)$ where Δ is the opening displacement along the load line. This displacement is measured by the clip-gauge shown. The gauge is of high sensitivity; it is made of high strength steel with strain gauge sensors and mounted in knife-edge supports (razor blades attached to the specimen fit into sharp V-grooves in the clip gauge).

Tests were performed on an Instron closed-loop servohydraulic test machine. Amounts of stable crack growth were estimated according to the elastic unloading compliance technique described by Clarke *et al.*;[10] elastic rotations were assumed to be given by their expression

$$\theta^e = 16(1-\nu^2)M/Eb^2. \quad . \quad . \quad . \quad . \quad . \quad . \quad . \quad . \quad . \quad . \quad . \quad (12)$$

The accuracy of the measurement of small changes in crack length (i.e. based on the ligament b inferred from equation (12) from the response to small increments of elastic unloading) is increased by the use of low-noise high-gain electronic instrumentation amplifiers to process P versus Δ records, and by minimization of friction. The latter is accomplished partly through design of the clip gauge and partly through the use of flexible hanger plates which allow the loading pins to rotate in needle bearings. This makes possible the resolution of inferred changes in crack size of the order of 0·01 mm.

Figure 4 shows a P versus Δ record for specimen 2. This is representative of all the specimens and illustrates the elastic unloading and reloading to infer crack growth.

The crack growth estimated by the compliance technique is compared to visually observed growth in Table 2. Here

Table 2 Comparison of maximum amount of crack growth in each test as estimated from changes in elastic compliance with actual growth observed visually from markings on fracture surface due to fatigue load cycling at end of test

Specimen number	Estimate from compliance changes, mm	Visual observation of load-cycle markings, mm
1	6·6	6·3
2	7·3	7·0
3	6·8	7·3
4	12·0	11·8

the values reported in the middle column are the total compliance-estimated growth at the end of the tests (e.g. when only 3–4 mm of ligament remained). Also, at the end of each test several cycles of fatigue loading were applied to mark the position of the crack front and then the thickness-average growth was measured visually, leading to results in the last column. The compliance-estimated growth is within 0·5 mm or less of the visually observed growth.

Experimental results for specimen 2 are shown in Fig. 5; the trend of the curves shown is representative of the results for all specimens. The horizontal axis denotes amount of crack growth and the curves labelled M and M_y denote, respectively, the applied moment and the fully plastic moment. The latter is calculated from[1,6] $M_y = 0{\cdot}364\sigma_y b^2$. Evidently, the early portion of the test corresponds to contained yielding and the later portion to general yielding. Also shown in Fig. 5 are the elastic energy release rates G calculated from

$$G = 16(1-\nu^2)M^2/Eb^3 \quad . \quad . \quad . \quad . \quad . \quad . \quad . \quad . \quad . \quad . \quad . \quad (13)$$

(which is consistent with equation (12)) and two different measures of quantities that can be associated with the J-integral, and which are discussed below.

The points denoted by the circular symbols in Fig. 5 give values of the 'deformation theory' value of J, namely J_d, in

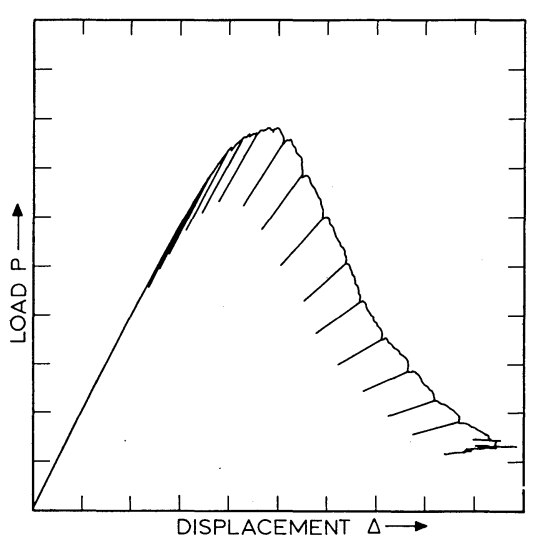

4 Load/displacement diagram for specimen 2 showing elastic unloading and reloading

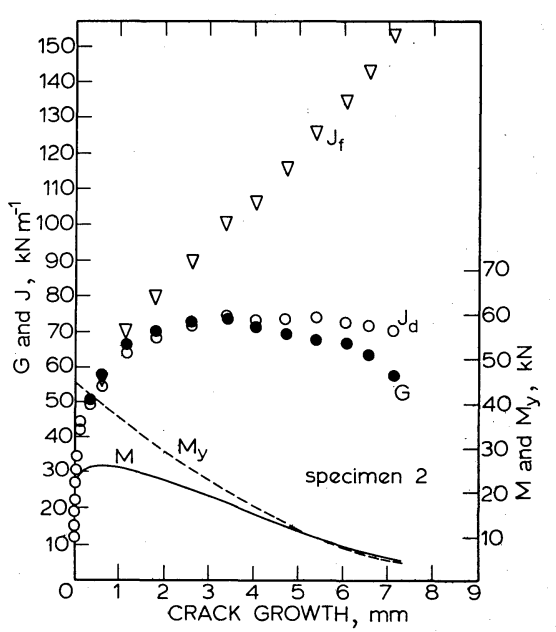

5 Applied moment M, general yield moment M_y, G, J_d, and J_f versus crack growth for specimen 2

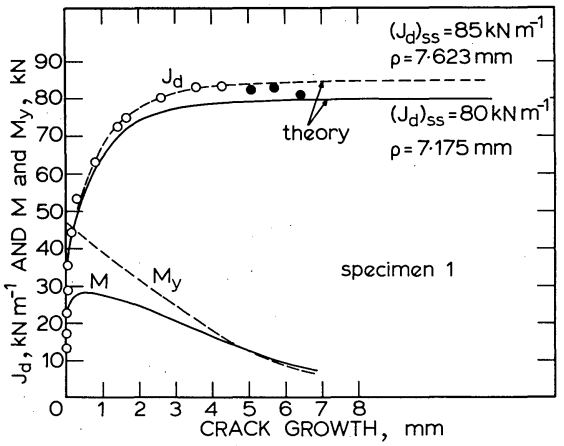

6 J_d (circular symbols) versus crack growth for specimen 1 and comparison with theoretical prediction

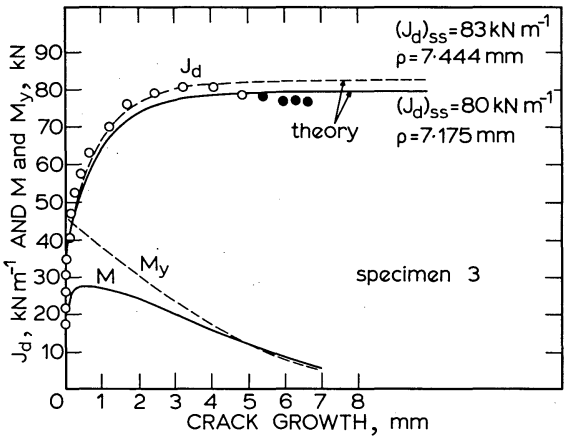

8 J_d (circular symbols) versus crack growth for specimen 3 and comparison with theoretical prediction

the terminology of Rice *et al.*[1] This is obtained by integrating

$$dJ_d = (2/b)M\,d\theta - (J_d/b)\,da$$
$$= (2/b)P\,d\Delta - (J_d/b)\,da. \quad (14)$$

throughout the test, starting at $J_d = 0$ when $\Delta = 0$. If the material were actually non-linear elastic then, as shown by Hutchinson and Paris,[11] the above expression when integrated for deeply cracked bend specimens defines a value J_d which depends only on the imposed deformation θ and the ligament size b and not on the 'path' by which the current values of θ and b were obtained. Further, J_d would then agree with the line-integral definition of J and reduce to $J_d = G$ in the limit of crack growth with a negligibly small non-linear zone. Similar independence of J_d from the path by which current θ and b values were obtained and agreement with line-integral values of J cannot be expected for actual elastic–*plastic* solids; in such cases J_d is merely *defined* by equation (14). On the other hand, it remains true that $J_d = G$ when a crack grows in an elastic–plastic solid with a negligibly small plastic zone. Indeed, it is clear from Fig. 5 that experimental results for J_d agree closely with those for G until the applied moment M approaches closely to M_y. In view of the properties of J_d, it seems most appropriate to associate J in equations (3) and (8) with J_d in order to use those equations at loads extending slightly beyond the limits of small-scale yielding.

The triangular symbols in Fig. 5 denote values of the 'far field' value of J, namely J_f, obtained by integrating

$$dJ_f = (2/b)M\,d\theta = (2/b)P\,d\Delta$$
$$= dJ_d + (J_d/b)\,da \quad (15)$$

throughout the test. The name 'far field' arises because, in the particular case of a deeply-cracked rigidly–ideally plastic bend specimen subject to monotonically increasing rotation, Rice *et al.*[1] showed that J_f thus defined agrees with the line-integral value of J as computed on a contour coinciding with the outer boundary of the specimen. There is no proof that a similar interpretation would be valid for *elastic*–plastic solids, or even for rigid–plastic solids in different specimen configurations. As noted above, certain definitions of J are consistent at general yielding with a continuing interpretation of R as a measure of the spatial extent of a region stressed in a fan-like manner. Others are not. As shown by Rice *et al.*[1] J_f has the proper features at full plasticity whereas J_d does not. (Later we shall consider another quantity which also exhibits the proper features at full plasticity and which reduces to $J \approx J_d \approx G$ at well contained yielding.) We observe from Fig. 5 that the difference between J_f and J_d is insignificant in the very early

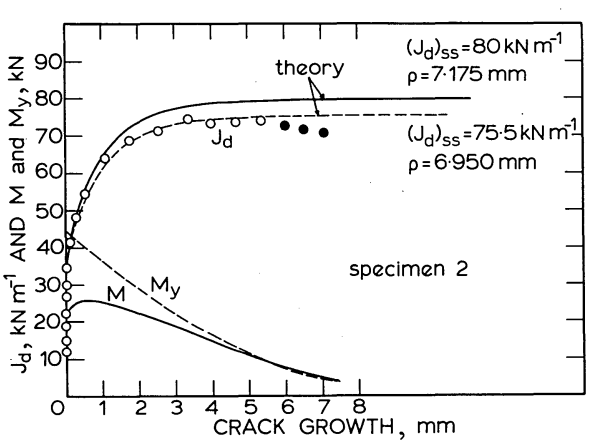

7 J_d (circular symbols) versus crack growth for specimen 2 and comparison with theoretical prediction

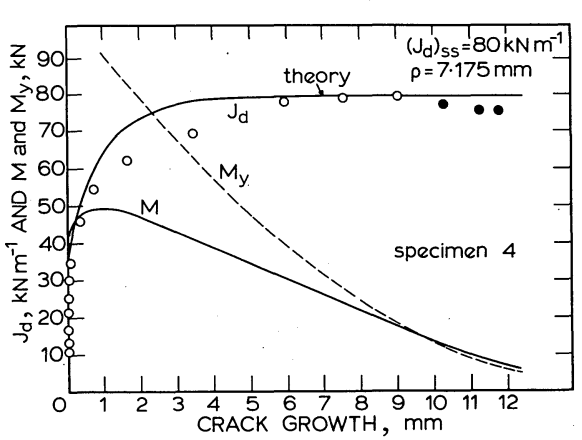

9 J_d (circular symbols) versus crack growth for specimen 4 and comparison with theoretical prediction

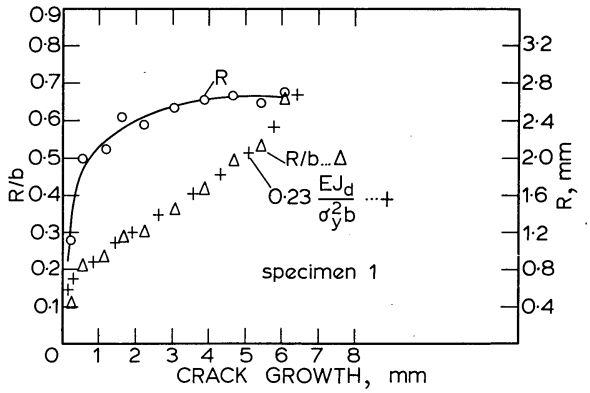

10 Inferred values of R and R/b versus crack growth for specimen 1 and comparison with predicted R/b value from small-scale yielding expression with J identified as J_d

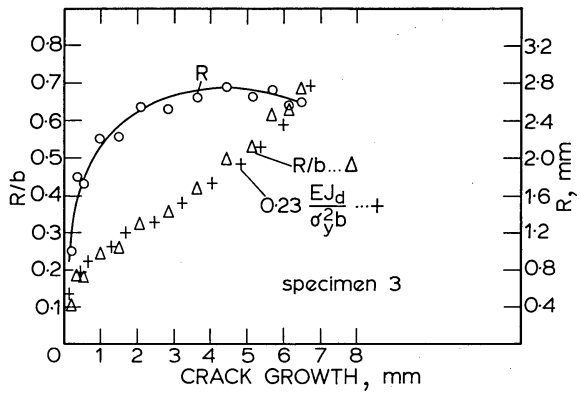

12 Inferred values of R and R/b versus crack growth for specimen 3 and comparison with predicted R/b value from small-scale yielding expression with J identified as J_d

stages of crack growth, but increasingly more significant with continuing growth. Also, it is evident from equation (15) that measurement of J_f versus a implies J_d versus a, and vice versa.

Figures 6–9 show, as circular symbols, the experimental results for J_d as a function of crack growth for specimens 1–4. The open circles are data points obtained prior to general yield (i.e. $M < M_y$) and the solid circles are results obtained after general yield. The solid and dashed curves represent the results of the theoretical prediction for well contained yielding.

COMPARISON OF EXPERIMENTS WITH SMALL-SCALE YIELDING FORMULATION

The theory is well developed only for crack growth under conditions of small-scale yielding. We show predictions of the theory for this case in Figs. 6–9, based on using J_d rather than G in the small-scale yielding formulation, and substituting σ_u or σ_y for σ_0 as discussed earlier. This formulation is given by combining equations (3) and (8) in the form (using $\beta = 5{\cdot}08$, $\alpha = \alpha_{ssy} = 0{\cdot}65$)

$$dJ_d/da = 7{\cdot}82(\sigma_u^2/E)\ln(\rho\sigma_y^2/0{\cdot}23eEJ_d) \quad . \quad . \quad . \quad . \quad . \quad (16)$$

This equation has been integrated subject to $J_d = 35$ kN m^{-1} at the onset of growth, as suggested by the data in Figs. 5–9, and values of the one free parameter ρ are chosen to best fit the data prior to general yield. Results are shown by the solid and dashed curves in Figs. 6–9.

The solid curves in Figs. 6–8 (specimens 1–3) are the same as the best-fit curve in Fig. 9. The value of ρ which generates this curve is $\rho = 7{\cdot}175$ mm, which implies that $(J_d)_{ss} = 80$ kN m^{-1}. The dashed curves in Figs. 6–8 correspond to slightly different values of ρ, giving the best fit for each specimen although the theory implies, of course, that ρ is a specimen-independent material property.

We conclude from Figs. 6–9 that the theory is reasonably successful in describing experimental data for crack growth prior to general yield.

FORMULATION FOR ARBITRARY EXTENT OF YIELDING

Here we present what we believe to be a plausible interpretation of the terms in the growth criterion of equation (8) for arbitrary amounts of crack growth and extent of yielding in deeply cracked bend specimens. The approach will, however, almost certainly be subject to revision when and if sufficiently accurate numerical elastic–plastic solutions become available to predict from first principles the relationship of terms in equation (8) to applied deformation and crack length.

First, consider the interpretation of dJ in the theoretical expressions. We can identify dJ as dG in the limit of growth with an extremely small non-elastic zone. On the other hand, dJ is subject to certain restrictions of interpretation as discussed earlier at large-scale and fully plastic yielding conditions. In particular, Rice *et al.*[1] show that for

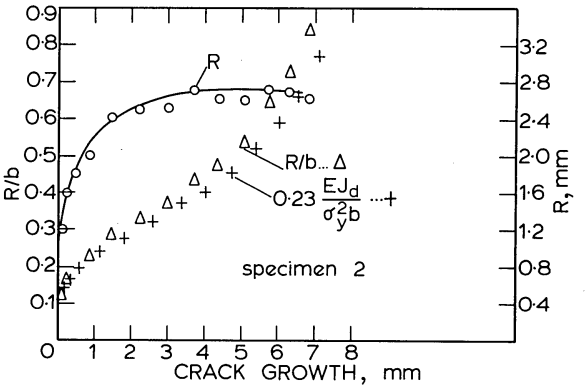

11 Inferred values of R and R/b versus crack growth for specimen 2 and comparison with predicted R/b value from small-scale yielding expression with J identified as J_d

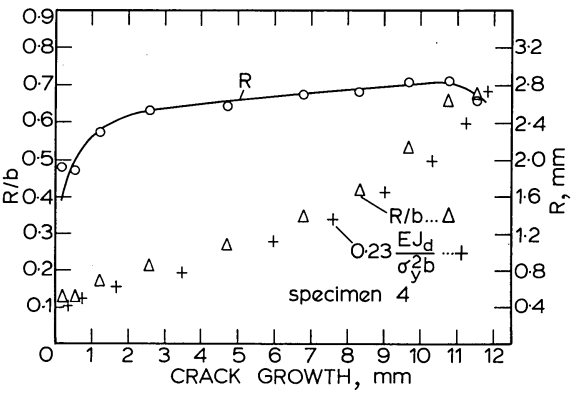

13 Inferred values of R and R/b versus crack growth for specimen 4 and comparison with predicted R/b value from small-scale yielding expression with J identified as J_d

rigid–ideally plastic bend specimens an expression $dJ = (2/b)M\,d\theta^p$, consistent with dJ_f of equation (14), is appropriate. Here $d\theta^p$ is the plastic part of the rotation. We can embody both limiting cases by writing

$$dJ = (2/b)M\,d\theta^p + dG \quad . \quad . \quad . \quad . \quad . \quad . \quad . \quad . \quad . \quad (17)$$

This can be rearranged by noting that $G = M\theta^e/b$ for a deeply-cracked bend specimen and that θ^e is given by equation (12). Thus

$$\begin{aligned} dG &= d[Eb(\theta^e)^2/16] \\ &= (2Eb\theta^e/16)\,d\theta^e + [E(\theta^e)^2/16]\,db \\ &= (2/b)M\,d\theta^e - (G/b)\,da \quad . \quad . \quad . \quad . \quad . \quad . \quad . \quad . \quad (18) \end{aligned}$$

by equation (12), and by using $db = -da$. Hence equation (17) can be written as

$$dJ = (2/b)M\,d(\theta^e + \theta^p) - (G/b)\,da$$

or

$$dJ = dJ_f - (G/b)\,da = dJ_d + [(J_d - G)/b]\,da \quad . \quad . \quad . \quad (19)$$

In terms of this interpretation of dJ the growth criterion of equation (8) may now be written as

$$dJ_d/da + (J_d - G)/b = (5{\cdot}08/\alpha)(\sigma_u^2/E)\ln(\rho/eR) \quad . \quad . \quad . \quad (20)$$

Here $\beta = 5{\cdot}08$ has been used and it is recognized that α should, in general, be regarded as variable.

We have used experimental data for J_d and G to evaluate the left-hand side of this equation, and by taking $\alpha = 0{\cdot}65$ and using the value of ρ from the small-scale yielding fit of the data we can infer R as a function of a from it. That is, we infer the variation of R with a on the assumption that the experimental data fit equation (20). The results are presented in Figs. 10–13 where we show R (right ordinate) and R/b (left ordinate) versus crack growth. Also, we show the value of R/b implied by the small-scale yielding expression of equation (3) when J_d is used for J.

We observe that R is rather well predicted by equation (3) throughout the range of these tests. This is probably a peculiarity of these experiments because equation (3) is not expected to be valid usually at general yielding. It was suggested in earlier work[1] that R/b should approach a limiting value as general yielding conditions are approached. Our experiments extend only modestly into the general yielding range and cannot provide a good test of this concept. However, the data which we have are not suggestive of an approach to a limiting value of R/b, at least over the range studied. Furthermore, the final R/b values in the experiments range from 0·6–0·8 and these seem rather large if R is to be interpreted as a size in the material over which fan-like stress fields such as those of Fig. 1 prevail. This topic requires further study, from both the standpoints of developing a suitable theoretical basis for growth in the general yielding range and of experimental analysis of the resulting growth criterion.

ACKNOWLEDGMENTS

The work was supported by the US Department of Energy under contract EY–76–S–02–3084 A003 with Brown University. We are grateful to Professor R. J. Asaro for helpful discussions and for his and Mr L. C. Majno's assistance with the heat treatment and we wish to thank Mr R. E. Dean for assistance with specimen preparation.

REFERENCES

1. J. R. RICE, W. J. DRUGAN, and T. L. SHAM: Proc. ASTM 12th Annual Symp. on 'Fracture mechanics', May 1979, ASTM–STP 700, 1980, 189–221.
2. J. R. RICE and E. P. SORENSEN: *J. Mech. Phys. Solids*, 1978, **26**, 163.
3. J. R. RICE and M. A. JOHNSON: 'Inelastic behavior of solids', (ed. M. F. Kanninen *et al.*), 641–671; 1970, New York, McGraw-Hill.
4. R. M. McMEEKING: *J. Mech. Phys. Solids*, 1977, **25**, 357.
5. R. M. McMEEKING and D. M. PARKS: 'Elastic–plastic fracture', (ed. J. D. Landes *et al.*), ASTM STP 668, 1979, 175–194.
6. J. R. RICE: 'Mechanics and mechanisms of crack growth', (ed. M. J. May), Br. Steel Corp. Phys. Met. Cent. Publ., 1973 (issued 1975), pp. 14–39.
7. D. M. PARKS: *Comp. Meth. Appl. Mech. Engr.*, 1977, **12**, 353.
8. C. F. SHIH: *J. Mech. Phys. Solids*, in press.
9. R. H. DEAN and J. W. HUTCHINSON: Ref. 1, 383–405.
10. G. A. CLARKE, W. R. ANDREWS, P. C. PARIS, and D. W. SCHMIDT: 'Mechanics of crack growth', ASTM STP 590, 1976, 27–42.
11. J. W. HUTCHINSON and P. C. PARIS: Ref. 5, pp. 37–65.